

Graphene Oxide/Multiwalled Carbon Nanotubes Composites as an Enhanced Sensing Platform for Voltammetric Determination of Salicylic Acid

Limin Lu^{1,2†}, Xiaofei Zhu^{1,2†}, Xinlan Qiu¹, Haohua He^{1,*}, Jingkun Xu^{2,*}, Xiaoqiang Wang¹

¹Key Laboratory of Crop Physiology, Ecology and Genetic Breeding, Ministry of Education, Jiangxi Agricultural University, Nanchang 330045, PR China

²Jiangxi Key Laboratory of Organic Chemistry, Jiangxi Science and Technology Normal University, Nanchang 330013, PR China

[†]These authors contributed equally to this work and should be considered co-first authors.

*E-mail: hhuua64@163.com; xujingkun@tsinghua.org.cn

Received: 30 September 2014 / Accepted: 22 October 2014 / Published: 28 October 2014

In this paper, a study of the electrocatalytic oxidation of salicylic acid (SA) at graphene oxide/multiwalled carbon nanotubes (GO/MWCNTs) modified electrode is presented. Compared to GO or MWCNTs electrodes, the electro-oxidation of SA significantly enhanced at the GO/MWCNTs electrode, accounting for the synergistic effect of MWCNTs and GO, in which MWCNTs increased the electronic conductivity and GO provided a large specific surface area to increase the loading amount of SA. Then the GO/MWCNTs electrode was applied for the electrochemical determination of SA in PBS at pH 6.5. Under the optimized conditions, the oxidation peak current was proportional to SA concentration in the range of 0.08 μM to 150 μM with a detection limit of 0.03 μM (S/N = 3). Moreover, the modified electrode showed high selectivity, good stability and reproducibility.

Keywords: Salicylic acid; Graphene oxide; Carbon nanotubes; Sensor; Determination

1. INTRODUCTION

Salicylic acid (SA), known as o-hydroxybenzoic acid, is one of an organic micro-molecular compound. As a phytohormone, it is widely distributed in various plants and acted as an endogenous signaling molecule, playing an important role in the regulation of many physiological processes such as flowering, heat production, seed germination, stomatal closure, membrane permeability and ion absorption [1]. Therefore, it is necessary to develop methods to quantify the concentration of SA in plants. Up to date, various methods have been used to detect SA, such as high performance liquid chromatography [2], gas chromatography-mass spectrometry [3], flow injection atomic absorption

spectrometry [4] and UV spectrophotometry [5] and electrochemical techniques [6]. Of these approaches, electrochemical method is emerging as a powerful approach due to the good electrochemical activity of SA as well as high sensitivity and simplicity of the method. Recently, different electrode systems have been explored for electrochemically detecting SA, such as Pt or Au electrodes [6] and Cu nanoparticles modified electrode [7], however, the existing reports need rather extreme pH conditions for the catalytic oxidation of SA. Therefore, it is crucial to explore electrochemical methods to detect SA at mild conditions with better analytical performance.

In recent years, there has been a rush of interest in graphene due to its intrinsic favorable properties, such as high electrical conductivity, large specific surface area and good biocompatibility [8,9]. As an important derivative of graphene, graphene oxide (GO) also has a similarly good performance to graphene owing to its high adsorption capacity, large surface area and good biocompatibility. In particular, GO contains a large number of hydrophilic functional groups, such as -OH, -COOH and epoxides on the basal plane and the sheet edge [10], which makes it show good hydrophilicity and can be easily dispersed in solvents with long-term stability. Based on the advantages mentioned above, GO-based electrochemical sensors have been developed for the sensitive determination of various biological molecules [11-13]. However, pristine GO exhibited weak catalytic performance in some cases due to its poor conductivity. Then different approaches have been used to improve its conductance. Among them, mixing GO with other conducting materials may provide an efficient way to improve its electrochemical performance. As one-dimensional nanomaterials, MWCNTs have generated great interesting applications based on their field emission and electronic transport properties, their high mechanical strength, high-surface to volume ratio and their chemical properties [14]. Combining GO with MWCNTs can not only effectively disperse MWCNTs, but also bring in new or enhanced functions through combining their individual characteristics [15,16]. However, to the best of our knowledge, electrochemical determination of SA using GO/MWCNTs modified electrode has not been reported.

In this work, GO/MWCNTs composite was prepared by a simple sonication mixing method and used as electrochemical sensor platform for the detection of SA. Based on the strong synergistic effect between GO and MWCNTs, the composites exhibited good promotion to the electrochemical oxidation of SA in a mild condition (PBS 6.5) and it could produce a sensitive anodic peak at GO/MWCNTs modified electrode. Under the optimal conditions, the peak current of SA was linear to its concentration in the range of 0.08 μM to 150 μM with a detection limit of 0.03 μM . The sensor presents fast response, low limits of detection, and excellent selectivity, which can open up new opportunities for fast, simple and sensitive detection of SA in real sample analysis.

2. EXPERIMENTAL

2.1. Chemicals and reagents

SA was purchased from Aldrich. Stock solution (5×10^{-3} M) was prepared with absolute ethanol. MWCNTs (purity > 95 %) were obtained from Shenzhen Nanotech Port Co. Ltd. Disodium hydrogen phosphate dodecahydrate (Na_2HPO_4), and sodium dihydrogen phosphate dehydrate (NaH_2PO_4) were

obtained from Sinopharm chemical reagent Co. Ltd. All other reagents were of analytical grade. Double distilled water was used throughout the experiments.

2.2. Apparatus

UV/vis spectra analysis was performed using a Perkin-Elmer Lambda 900 ultraviolet-visible-near-infrared spectrophotometer (Germany). SEM images were obtained at a JSM-6701F scanning electron microscope. Electrochemical measurements were carried out on CHI 660D electrochemical workstation (Shanghai, China). A conventional three-electrode cell was used with a GCE (with a diameter of 3 mm) as the working electrode, a platinum wire as the counter electrode and a saturated calomel electrode (SCE). Except the specific statement, the electrochemical measurements were carried out in 0.1 M PBS (pH 6.5) at room temperature (25 ± 4 °C).

2.3. Preparation of GO/MWCNTs and fabrication of GO/MWCNTs /GCE

GO was synthesized from natural graphite powder according to a modified Hummers method [17]. The GO/MWCNTs suspension was prepared by adding 0.5 mg GO and 1 mg pristine MWCNTs to 1 ml deionized water. A stable black suspension was obtained by ultrasonication for 2 h.

Prior to modification, the GCEs were mechanically polished with chamois leather containing 0.05 μm alumina slurry, rinsed thoroughly with double distilled water, and then it was ultrasonically cleaned with doubly distilled water, absolute ethanol and doubly distilled water each for 5 min, respectively, finally dried in air before use. To obtain GO/MWCNTs modified GCE, 5 μL of the above-mentioned suspension was dropped on the surface of GCE in air at room temperature. For comparison, the MWCNTs/GCE and GO/GCE were also prepared with the same method.

3. RESULTS AND DISCUSSION

3.1. Characterization of the synthesized GO/MWCNTs/GCE

The morphologies and microstructures of the GO, MWCNTs and GO/MWCNTs were investigated by means of SEM (Fig. 1). It was found that GO exhibited crumpled and wrinkled flake like structure (A), while large quantities of MWCNTs were well distributed within the film and most of the MWCNTs were in the form of small bundles with 40 - 60 nm in diameter (B). However, it can be seen that the extent of aggregation and number of junctions between MWCNTs in GO/MWCNTs (C) hybrid film were clearly reduced compared to raw MWCNTs, which can be attribute to the excellent dispersing ability of GO. It was also noted that the nanohybrid showed relatively rough surface and possessed distinct interstices morphology. This special structure could greatly increase the surface-to-volume ratio and be highly efficient to capture more SA, thus the response properties of the prepared sensor would be greatly improved.

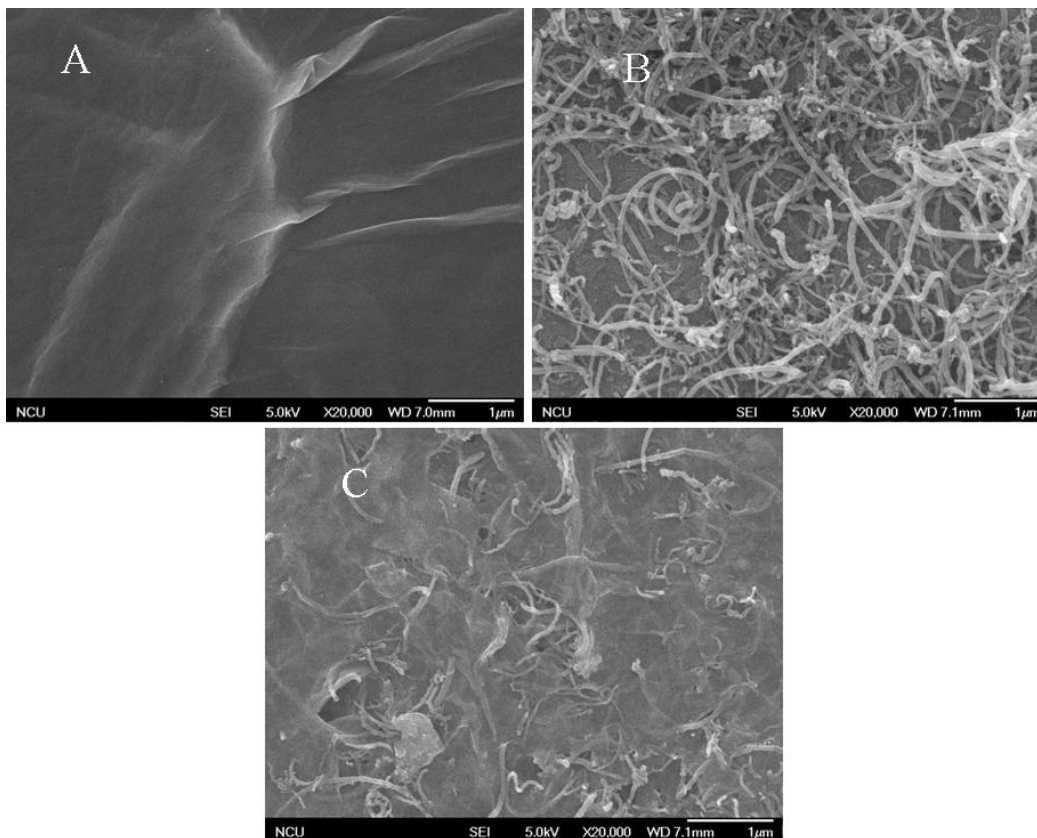


Figure 1. SEM images of GO (A), MWCNTs (B) and GO/MWCNTs (C).

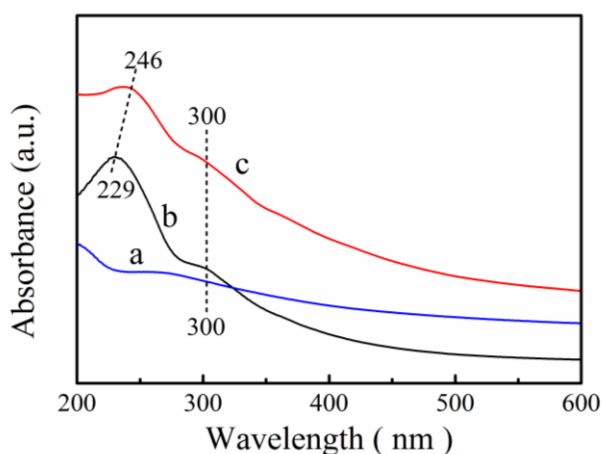


Figure 2. UV-vis absorption spectra of MWCNTs (a), GO (b) and GO/MWCNTs (c).

Fig. 2 shows the UV-vis spectrum of MWCNTs (a), GO (b) and GO/MWCNTs (c). As can be seen, there was no obvious absorption on the MWCNTs (a). While GO exhibited two characteristic absorption peaks, an absorption peak at 229 nm and a shoulder peak at 300 nm (b). The peak at 230 nm was due to the $\pi - \pi^*$ transition of the C – C bonds in the aromatic region of GO sheets and the latter one was due to the $n - \pi^*$ transition in the C = O bonds of the functional groups. However, the $\pi - \pi^*$ transition of GO appeared at 229 nm was red shifted to higher wavelength of 246 nm

(Bathochromic shift) and no noteworthy shift has been observed for the $n - \pi^*$ transition in the spectrum of GO/MWCNTs (c). Hence, the interaction should be $\pi - \pi$ stacking interaction via hydrophobic aromatic regions between MWCNTs and the aromatic basal plains of GO. These results indicated that GO/MWCNTs composites have been successfully prepared by ultrasonic mixing.

Electrochemical impedance spectra (EIS) has been reported as an effective method to monitor the features of a surface to allow the understanding of chemical transformations and processes associated with the conductive electrode surface [18]. The curve of EIS present as Nyquist plot consists two parts: a semi-circle part at higher frequency range and a straight line part at lower frequency range, which are corresponding to the electron transfer-limit process and diffusion-limit process, respectively. Fig. 3 shows the EIS of bare (a), GO (b), MWCNTs (c) and GO/MWCNTs (d) (inset of Fig. 3) modified GCEs in the presence of 5 mM $[\text{Fe}(\text{CN})_6]^{4-/3-}$ solution. As can be seen, bare GCE exhibited a depressed semicircle with a R_{ct} value of 410 Ω (a). While GO modified GCE showed a R_{ct} value of 6980 Ω (b), indicating the hindered electron transfer at GO modified electrode. By contrary, a depressed semicircle with smaller diameter (with an R_{ct} value of 28 Ω) was observed at MWCNTs/GCE (c), validating its high conductivity and fast electron conducting ability at the electrode surface. Whereas, one can see that the semicircle diameter of GO/MWCNTs/GCE (with an R_{ct} value of 125 Ω) (d) was larger than that of MWCNTs/GCE. This phenomenon was probably due to the fact that the negatively charged functional groups on GO sheets repelled the negatively charged $[\text{Fe}(\text{CN})_6]^{4-/3-}$ probe [19]. EIS results clearly validates that the GO/MWCNTs composite has excellent conductivity and good electron transfer, which can be ascribed to the fact that MWCNTs act as a good conduit between GO and electrode surface.

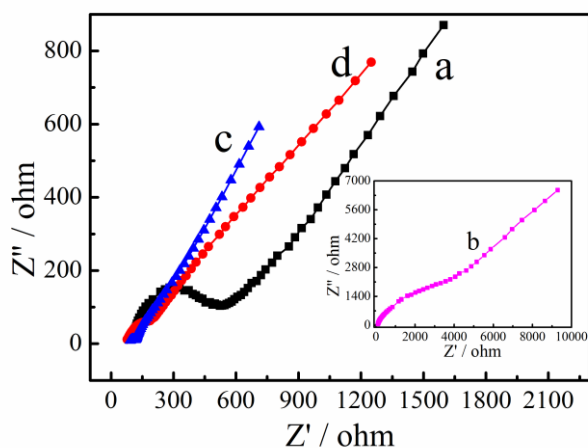


Figure 3. The impedance spectrum of GCE (a), GO/GCE (b), MWCNTs/GCE (c) and GO/MWNTs/GCE (d) in 5 mM $\text{Fe}(\text{CN})_6^{3-/4-}$ (1:1) solution containing 0.1 M KCl.

3.2. Cyclic voltammetric studies of GO/MWCNTs /GCE

Cyclic voltammetric responses of SA at the bare GCE (a), GO/GCE (b), MWCNTs/GCE (c) and GO/MWCNTs/GCE (d) in the presence of 150 μM SA (PBS, pH 6.5) were shown in Fig. 4. As

can be seen, there were no clear redox peaks on bare GCE and GO/GCE, which might be due to the sluggish electron transfer of GCE and low conductivity of GO. However, an obvious and irreversible oxidation peak at 0.95 V can be seen on MWCNTs/GCE, which might be attributed to the large surface area and high conductivity of MWCNTs. Compared with MWCNTs/GCE, the oxidation peak current strengthened again and showed more negative potentials (0.91 V) at GO/MWCNTs/GCE. The reasons for the increased peak currents of the SA oxidation at the GO/MWCNTs/GCE may be summarized as follows: (1) MWCNTs increased the electronic conductivity and the network structure of GO provided a large specific surface area to increase the loading amount of SA [20,21]. (2) The well-distributed GO sheets on the surface of MWCNTs had very strong adsorptive capability for SA due to several interactions, including hydrogen bonds, hydrophobic force and electrostatic interaction [22,23].

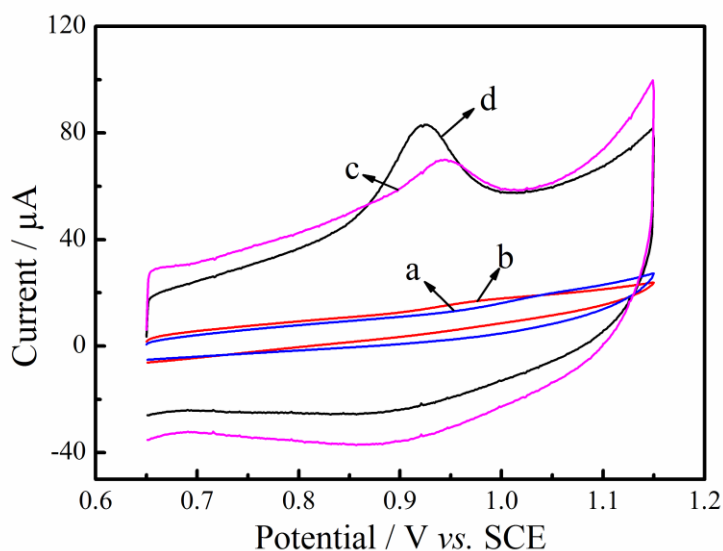


Figure 4. Cyclic voltammograms of 150 μM SA in 0.1 M PBS (pH 6.5) at the bare GCE (a), GO/GCE (b), MWCNTs/GCE (c) and GO/MWCNTs/GCE (d) at the scan rate of 50 mV s^{-1} . Accumulation time: 40 s.

3.3. Effect of accumulation time

It is stated that accumulation time had a remarkable effect on peak current, it is necessary to investigate the influence of accumulation time. In this experiment, the effect of accumulation time was also investigated in 8 μM SA solution (PBS 6.5). As can be seen in Fig. 5, the oxidation peak current of SA reached a maximum after 40 s and then stabilized, indicating that 40 s was sufficient to reach the SA saturation in the GO/MWCNTs/GCE. Considering both sensitivity and work efficiency, 40 s was employed in the further experiments.

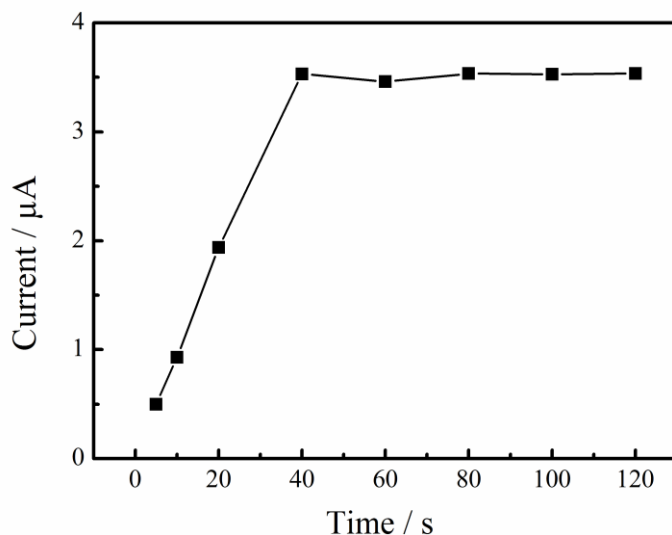


Figure 5. Variation of the peak current with accumulation time in 0.1 M PBS (pH 6.5). SA concentration: 8 μM . Scan rate: 50 mV s^{-1} .

3.4. Effect of scanning rate

The effect of scan rate on the electro-oxidation of SA at GO/MWCNTs/GCE was investigated by cyclic voltammetry. The cyclic voltammograms of 10 μM SA at GO/MWCNTs/GCE were recorded at different scan rates. From Fig. 6A, it can be seen that the peak currents (I_{pa}) increase linearly with the scan rate (ν) in the range of 10 – 300 mV s^{-1} . The linear regression equation can be expressed as $I_{\text{pa}} = 0.0860 \nu + 1.7409$ ($R^2 = 0.9995$), indicating that the oxidation of SA is an adsorption-controlled electrode process [24]. Similarly, a linear relationship between E_{pa} and Napierian logarithm of ν ($\ln \nu$) was also observed in the range of 10 – 25 mV s^{-1} (Fig. 6B) and the linear regression equation can be expressed as $E_{\text{pa}} = 0.8596 + 0.0173 \ln \nu$ ($R^2 = 0.9892$). As for a totally irreversible and adsorption-controlled electrode process, E_{pa} could be defined by the equation as follows [25]:

$$E_{\text{pa}} = E^0 + (RT/\alpha nF) \ln (RTk^0/\alpha nF) + (RT/\alpha nF) \ln \nu$$

Where k^0 is standard rate constant of the reaction, α is transfer coefficient, n is electron transfer number involved in rate-determining step, E^0 is formal redox potential, ν is scan rate, other symbols have their usual meanings. Based on the linear correlation of E_{pa} versus $\ln \nu$ as mentioned above, the slope of the line is equal to $RT/\alpha nF$, therefore the value of αn was calculated to be 1.49. Generally, α is assumed to be 0.5 in totally irreversible electrode process [24], thus the electron transfer number (n) is around 3. The standard heterogeneous rate constant (k_s) for totally irreversible oxidation of SA at the GO/MWCNTs/GCE was calculated based on Velasco equation [26]:

$$k_s = 2.415 \exp(-0.02 F/RT) D^{1/2} (E_{\text{pa}} - E_{\text{pa}/2})^{-1/2} \nu^{1/2}$$

where $E_{\text{pa}/2}$ represents the potential at which $I = I_{\text{pa}/2}$, D is diffusion coefficient, for SA, it is $1.11 \times 10^{-5} \text{ cm}^2 \text{ s}^{-1}$ [27], other symbols have their usual meanings. Therefore, k_s was calculated to be $7.6 \times 10^{-2} \text{ cm s}^{-1}$.

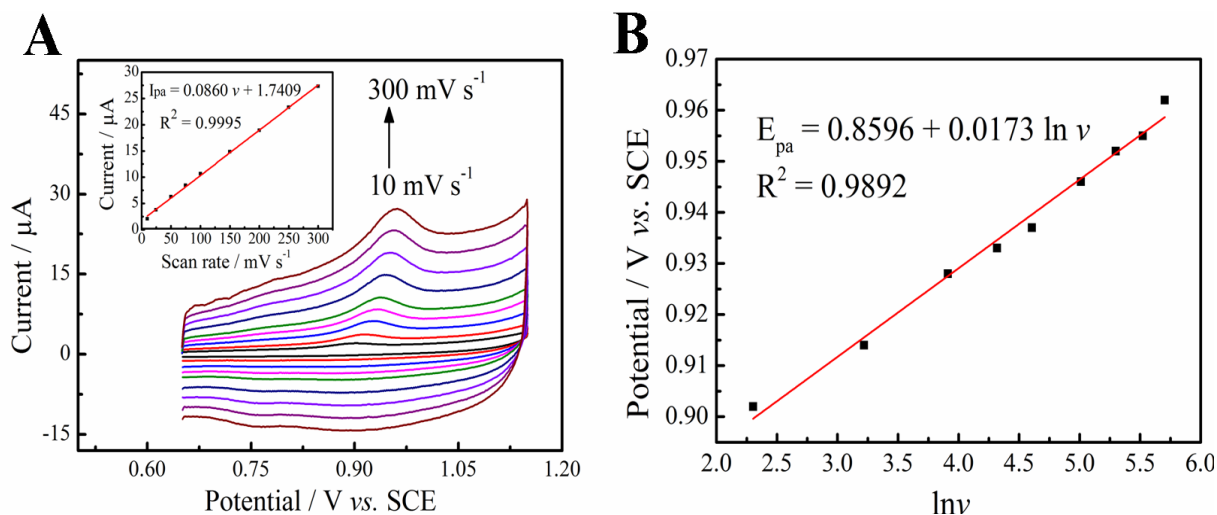


Figure 6. (A) Cyclic voltammograms of 10.0 μM SA with different scan rates (ν) on GO/MWCNTs/GCE in pH 0.1 PBS (pH 6.5) (from the inner to the outer are 10, 25, 50, 75, 100, 150, 200, 250, 300 mV s^{-1} , respectively). (B) The relationship between E_{pa} and natural logarithm of potential scan rate.

3.5. Determination of salicyl acid (SA)

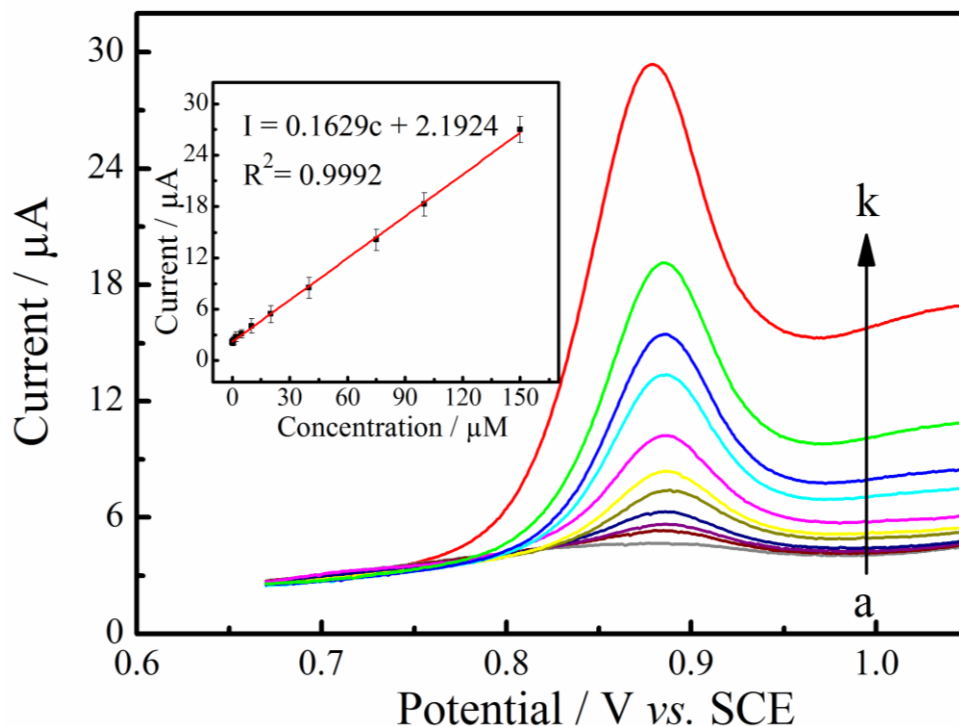


Figure 7. DPVs of 0.08, 0.1, 0.5, 0.9, 2, 5, 10, 20, 40, 75, 100 and 150 μM SA on GO/MWCNTs/GCE. Inset of Figure 7: plot of the oxidation peak current against the concentration of SA. Other conditions are the same as Figure 4.

The differential pulse voltammetry (DPV) could significantly improve the sensitivity and detection limits of electrochemical measurements by decreasing the effect of the charging current. Therefore, DPV was performed to investigate the relationship between the oxidation peak current and the concentration of SA at the proposed electrochemical sensor under the optimal conditions. Fig. 7 depicts the DPV curves of SA at various concentrations. As can be seen in the insert of Fig. 7, the reduction peak current has a good linear relationship with the SA concentration in the range from 0.08 μM to 150 μM . The linear regression equation was $I (\mu\text{A}) = 2.1924 + 0.1629 c (\mu\text{M})$ ($R^2 = 0.9992$). The detection limit was estimated to be about 0.03 μM , which is lower than that obtained on graphite-epoxy-composed electrode (5 μM) [28], multiwalled carbon nanotube electrode (0.8 μM) [29] and Au@Fe₃O₄ nanocomposites modified electrode (0.1 μM) [30]. The lower detection limit could be attributed to the combination of MWCNTs and GO, in which MWCNTs increased charge transport and GO provided a large specific surface area to increase the loading of SA. These results indicated that GO/MWCNTs/GCE was an appropriate platform for the determination of SA.

3.6. Reproducibility, repeatability, stability, and interference study

The reproducibility and repeatability of the GO/MWCNTs electrode were examined at 50 μM SA, the relative standard deviation (R.S.D.) for eight successive measurements was 3.7 %, and the R.S.D. of five electrodes made independently was 4.1 %. Moreover, the modified electrode retained more than 95% of its initial sensitivity to the oxidation of SA which have been stored at 4 °C for 1 week. The results indicated that the GO/MWCNTs electrode possessed good repeatability, reproducibility and stability.

The influences of some common ions and electrochemically active phenols similar to SA on the determination of SA (50 μM) were studied in the experiment under the optimal experimental conditions. The results indicated that the concentration of 10 times of K⁺, Na⁺, Cu²⁺, Cl⁻, NO₃⁻; 20 times of Mg²⁺, Zn²⁺, 50 times of SO₄²⁻ and 500 times of CH₃CH₂OH did not affect the determination of SA. Moreover, the results also shows that 1,4-diphenol, sucrose in the double concentration did not interfere the detection with the peak current changes less than $\pm 5\%$, suggesting that the proposed method has a good anti interference ability.

4. CONCLUSION

In this work, nanocomposites of GO and MWCNTs have been prepared and dropped on the glassy carbon electrode to form the GO/MWCNTs modified electrodes. The composite modified electrode showed enhanced electron transfer properties and favorable electrocatalytic performance to SA in a mild condition. Moreover, the fabricated electrode had wider linear range and lower detection limit, and it also exhibited good stability and reproducibility, indicating the composite could be used as a promising sensing platform for SA determination.

ACKNOWLEDGEMENTS

This work was supported by the National Natural Science Foundation of China (50963002, 51073074, 51272906, 51263010), Natural Science Foundation of Jiangxi Province (2010GZH0041, 20122BAB213007), Jiangxi Provincial Department of Education (GJJ11590, GJJ10678, GJJ13258) and Postdoctoral Science Foundation of China (2014M551857).

References

1. Z. Wang, F. Ai, Q. Xu, Q. Yang, J. Yu, W.H. Huang, Y.D. Zhao, *Colloid Surf. B.* 76 (2010) 370.
2. X.Y. Long, F.N. Chen, M. Deng, *Anal. Sci.* 29 (2013) 227.
3. P. Lacina, L. Mravcova, M. Vavrova, *J. Environ. Sci. China.* 25 (2013) 204.
4. G.A. Rivas, J.M. Calatayud, *Talanta.* 42 (1995) 1285.
5. I.M. Scott, H. Yamamoto, *Phytochemistry.* 37 (1994) 335.
6. A.A. Torriero, J.M. Luco, L. Sereno, J. Raba, *Talanta.* 62 (2004) 247.
7. Z. Wang, F. Wei, S.Y. Liu, Q. Xu, J.Y. Huang, X.Y. Dong, J.H. Yu, Q. Yang, Y.D. Zhao, H. Chen, *Talanta.* 80 (2010) 1277.
8. M.J. Allen, V.C. Tung, R.B. Kaner, *Chem Rev.* 110 (2010) 132.
9. L.H. Tang, Y. Wang, Y.M. Li, H.B. Feng, J. Lu, J.H. Li, *Adv Funct Mater.* 19 (2009) 2782.
10. S. Stankovich, D.A. Dikin, R.D. Piner, K.A. Kohlhaas, A. Kleinhammes, Y.Y. Jia, *Carbon.* 45 (2007) 1558.
11. Y. Wang, Y. Li, L. Tang, J. Lu, J. Li, *Electrochem. Commun.* 11 (2009) 889.
12. J.Y. Sun, K.J. Huang, S.Y. Wei, Z.W. Wu, F. Ren, *Colloid Surf. B.* 84 (2011) 421.
13. M.S. Goh, M. Pumera, *Anal. Bioanal. Chem.* 399 (2011) 127.
14. R.R. Gaichore, A.K. Srivastava, *Sensor Actuat B-chem.* 188 (2013) 1328.
15. S.H. Aboutalebi, A.T. Chidembo, M. Salari, K. Konstantinov, D. Wexler, H.K. Liu, S.X. Dou, *Energy Environ. Sci.* 4 (2011) 1855.
16. J.H. Li, D.Z. Kuang, Y. Feng, F. Zhang, Z.F. Xu, M.Q. Liu, D.P. Wang, *Microchim Acta.* 180 (2013) 49.
17. K. Zhang, L. Zhang, X.S. Zhao, *J Mater Chem.* 22 (2010) 1392.
18. J. J. Feng, G. Zhao, J. J. Xu, H. Y. Chen, *Anal. Biochem.* 342 (2005) 280.
19. Y.J. Yang, W. Li, *Biosens Bioelectron.* 56 (2014) 300.
20. S.H. Aboutalebi, A.T. Chidembo, M. Salari, *Energ Environ Sci.* 4 (2011) 1855.
21. Li Y, Yang T, Yu T, et al. *J Mater Chem.* 21 (2011) 10844.
22. C. Wu, D. Sun, Q. Li, K.B. Wu, *Sensor Actuat B-chem.* 168 (2012) 178.
23. M. Arvand, T.M. Gholizadeh. *Sensor Actuat B-chem.* 186 (2013) 622.
24. A.J. Bard, L.R. Faulkner, *Electrochemical Methods: Fundamentals Applications*, second ed., Wiley, New York, 1980.
25. E.L. Adsorption, *J Electroanal Chem.* 52 (1974) 355.
26. J.G. Velasco, *Electroanalysis.* 9 (1997) 880.
27. J.M. Delgado, *J. Phase Equilib. Diff.* 28 (2007) 427.
28. Y. Zhu, X.Y. Guan, H.G. Ji, *J Solid State Electrochem.* 13 (2009) 1417.
29. W.D. Zhang, B. Xu, Y.X. Hong, Y.X. Yu, J.S. Ye, J.Q. Zhang. *J Solid State Electrochem.* 14 (2010) 1713.
30. L.J. Sun, Z.Q. Pan, J. Xie, X.J. Liu, F.T. Sun, F.M. Song, N. Bao, H.Y. Gu. *J Electroanal Chem.* 706 (2013) 127.